

# Loop Heat Pipe Wick Fabrication via Additive Manufacturing

Bradley Richard<sup>1</sup>, Devin Pellicone<sup>2</sup>, and Bill Anderson<sup>3</sup>  
*Advanced Cooling Technologies, Inc., Lancaster, PA, 17601*

As the capabilities of CubeSats and SmallSats increase so do the heat rejection requirements. While loop heat pipes (LHPs) are capable of transporting heat across deployable radiators they are currently too expensive for most applications. The largest cost comes from the fabrication of the primary wick which requires multiple machining steps as well as a knife-edge seal. The focus of this work is the development of a 3D printed LHP evaporator using a direct metal laser sintering (DMLS) process to fabricate the primary wick. 3D printing LHP wicks offer several advantages. The overall cost can be significantly reduced by eliminating multiple machining steps, and the risk of failure can be reduced by eliminating the knife-edge seal. The challenge with 3D printing of LHP primary wicks is that a very small pore radius is required to supply sufficient capillary pumping power. A pore radius study was conducted for optimization of DMLS methods and parameters for fabricating primary wicks. The result of this study is DMLS parameters for wicks with pore radii less than 10 $\mu$ m. In addition, a DMLS parameter optimization study was performed for fabrication of the coarser secondary wick. Experimental testing was completed on a complete LHP prototype with 3D printed primary wick fabricated using the optimized DMLS parameters. The LHP prototype demonstrated steady state operation at a power of 125W.

## Nomenclature

$P_b$  = bubble point pressure  
 $R_p$  = pore radius

$\sigma$  = surface tension

## I. Introduction

NASA's CubeSat and SmallSat programs provide the ability to rapidly develop and launch small scale satellite platforms for science research and technology demonstration uses, while reducing costs and increasing efficiency. Conventional spacecraft thermal control systems utilize constant conductance heat pipes (CCHPs) and encapsulated pyrolytic graphite for the passive transport of waste heat. However, pyrolytic graphite is very expensive, and CCHPs are difficult to test on the ground and are not generally used for deployable radiators. Loop heat pipes (LHPs) are another commonly utilized thermal control system for spacecraft, but the manufacturing costs are currently too high to make them viable for most CubeSat/SmallSat applications. In this work a low-cost LHP evaporator was fabricated using a technique called Direct Metal Laser Sintering (DMLS), otherwise known as 3D printing.

DMLS is a process by which metal structures are made in a layer-by-layer sintering process that selectively melts powdered metal. Geometries should complement the building process which favors upward slanting surfaces and large radii just under horizontal structures. Utilizing the DMLS process, metal parts of the most complex geometries are built layer-by-layer directly from 3D CAD models. Unique geometric freedom of design enables DMLS to form cavities and undercuts, which with conventional machining methods can only be produced with great difficulty, if at all. The metal powder is most often melted entirely to create a fully dense, homogenous structure. In the case of a LHP primary wick a porous part must be printed with a pore radius on the order of 1-10 $\mu$ m in order to have a high enough capillary pressure to overcome the total pressure drop of LHP. A porous part can be accomplished by adjusting the DMLS parameters so that complete melting does not occur, but pore sizes have been

<sup>1</sup> R&D Engineer, Custom Products Group, 1046 New Holland Ave. Lancaster, PA 17601.

<sup>2</sup> Lead Engineer, Custom Products Group, 1046 New Holland Ave. Lancaster, PA 17601.

<sup>3</sup> Chief Engineer, 1046 New Holland Ave. Lancaster, PA 17601.

limited to  $>50\mu\text{m}$ . In this work a small scale parameter study optimized DMLS parameters to produce porous wicks with pore radii  $<10\mu\text{m}$ .

The work presented in this paper is on the second generation 3D printed LHP prototype. The first generation prototype successfully demonstrated the ability to use DMLS to fabricate a primary wick. However, the pore radius of the primary wick was  $44\mu\text{m}$  which limited the maximum power before dry-out to only 45W. A more comprehensive DMLS parameter optimization study was required to reduce the pore size of 3D printed wicks to improve performance.

## II. Background

### A. Loop Heat Pipe Operation

LHPs are high thermal conductance devices that are self-contained and passive. Figure 1 shows a schematic of a LHP. Note that the figure is not to scale; the vapor and liquid lines can be made much longer. Heat enters the evaporator and vaporizes the working fluid at the interface between the wick and envelope. The vapor is collected by a system of grooves and headers. The vapor flows down the vapor line to the condenser where it condenses as heat is removed by the cold plate. Most of the condenser is filled with a two-phase mixture. A small section at the end of the condenser provides a small amount of liquid sub-cooling.

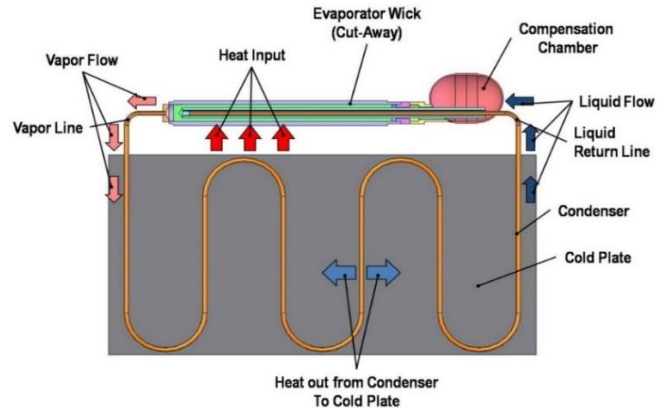


Figure 1. Loop heat pipe schematic (not to scale).

The compensation chamber (or reservoir) at the end of the evaporator is designed to operate at a lower temperature than the evaporator. The temperature of the compensation chamber can be used to control the operating temperature of the LHP. Since the temperature is lower, the pressure of the saturated fluid in the compensation chamber is also lower. This lower pressure draws the condensate through the condenser and the liquid return line<sup>2</sup>. The fluid then flows into a central pipe where it feeds the wick. Excess fluid drains into the compensation chamber. A secondary wick in the evaporator and compensation chamber allows the liquid in the compensation chamber to feed the evaporator wick. This communication between the compensation chamber and primary wick is required during transient operations. The liquid in the compensation chamber and the interior of the wick must be returned to the exterior surface of the wick to close the cycle. Capillary forces accomplish this passively, pulling liquid back to the surface, similar to water being absorbed into a sponge. Loop heat pipes are made self-priming by carefully controlling the volumes of the compensation chamber, condenser, vapor line and liquid line so that liquid is always available to the wick. The compensation chamber size and fluid charge are set so that there is always fluid in the compensation chamber even if the condenser, vapor line and liquid line are completely filled. The LHP is thus inherently self-priming.

### B. Loop Heat Pipe Fabrication

The key component of the Loop Heat Pipe system is the pump assembly and its corresponding subcomponents<sup>1</sup>. A detailed view of this assembly is shown in Figure 2. The key subcomponents of the pump assembly consist of the cylindrical envelope, a primary wick, a secondary wick, the bayonet, two bi-metallic transition couplings, and the Knife Edge Seal (KES). The compensation chamber is welded to this pump subassembly via one of the bimetallic transitions. The KES is critical for developing the differential pressure required to drive the working fluid around the system. The need for a KES and bi-metallic joints is a large source of the shortcomings associated with LHP evaporator production and reliability.

Currently, the primary wick structure is produced external from the envelope, using sintered Nickel powder. The fabrication process entails compacting Nickel powder into a sintering mandrel and firing at high temperatures. The oversize wick is then machined at low speeds, and without lubricant to produce the vapor grooves and reduce the outer diameter to the proper size while preventing contamination.

Once the primary wick structure is successfully produced, machined to the correct size, and hydrodynamically characterized, the insertion of the wick into the envelope takes place. With a slight interference fit at room

temperature between the primary wick and the evaporator body, the envelope must be heated to expand the inner diameter of the envelope. Then the wick is chilled to slightly reduce its diameter and inserted. The design of the wick and the interference fit theoretically results in intimate contact between all the circumferential grooves of the wick and the aluminum envelope. In practice, once the wick is installed the actual contact area is unknown. It is suspected that the physical insertion of the wick shaves and smears the circumferential grooves thereby reducing contact and subsequently the thermal performance of the assembly.

Once the primary wick structure is inserted into the envelope, the KES must be installed. A bi-metallic insertion piece with the knife edge features is evenly pressed into the sintered wick, creating a seal between the inner and outer regions of the primary wick. A bi-metallic interface is necessary because it is desirable to have a KES material with a higher hardness than compared to the Aluminum LHP envelope in order to maintain the integrity of the KES. Experience has shown that a proper seal is not always achieved, and if this KES insertion process fails and reinsertion is attempted, the primary wick is likely to become damaged. This damage typically requires the wick to be scrapped. The envelope may be reused but a new wick must be manufactured. It is also possible for the KES to pass verification testing after assembly but fail later after numerous thermal cycles or vibration testing.

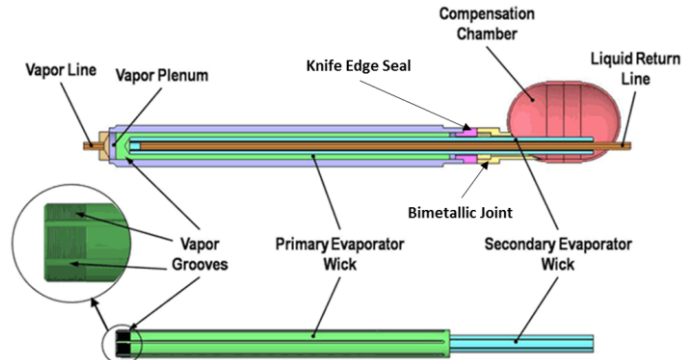


Figure 2. Detailed view of LHP evaporator

Once the bayonet and secondary wick subassembly are inserted down the bore of the primary wick, the next step in the LHP pump assembly is attaching the front end of the compensation chamber by welding to the bimetallics. This process is of concern, due to mismatches in the material coefficient of thermal expansion (CTE) in the Aluminum-Stainless Steel bimetallic transition coupling. Excessive heating of the coupling causes the materials to expand at different rates resulting in a significant stress at the two-material interface. The bimetallic coupling is an off-the-shelf component, and that interface is produced using a friction-stir welding process that has historically been shown to produce an excellent bond between dissimilar metals. However, excessive heating of this component has an inherent high level of risk and has resulted in part failure.

### III. Small Scale Parameter Study

#### A. Primary Wick

There are a couple of different techniques that can be used to produce a porous wick structure using a DMLS approach. One method is to design a lattice structure. This offers a high level of control, but is computationally expensive and the smallest pore size possible is limited by the accuracy and diameter of the laser. For primary wicks very small pore sizes on the order of 1-10 $\mu$ m are of interest so alternative methods were used. First the spacing between each laser path was increased as shown by DMLS Parameter Set 1 in Figure 3. The result is similar to a lattice structure without the need to have a detailed CAD model. The second approach investigated was adjusting the laser power to a level where the metal powder is sintered together, but not fully melted to form a fully dense part. The resulting wick as shown as DMLS Parameter Set 2 in Figure 3 is much closer to traditional wicks formed by sintering metal powder in a furnace.

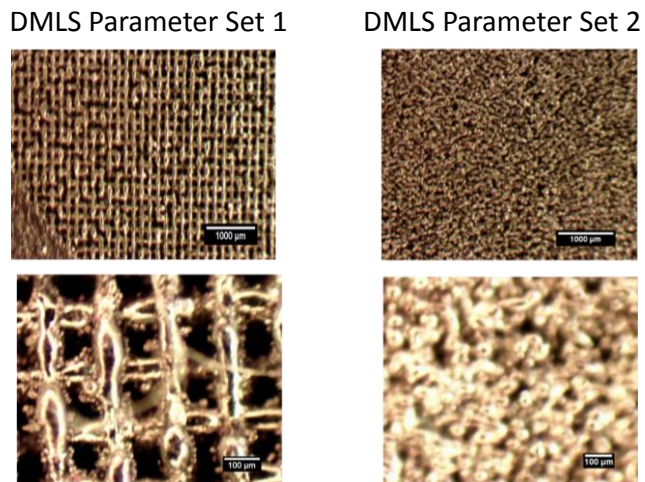


Figure 3. Images of 3D printed wicks showing two different methods of using DMLS to create porous structures

**Table 1. Small Scale Parameter Study Results**

| Sample | Pore Radius |
|--------|-------------|
|        | μm          |
| 1      | 6.2         |
| 2      | 5.6         |
| 3      | 11.6        |
| 4      | 10.3        |
| 5      | Hollow      |
| 6      | Solid       |
| 7      | Solid       |
| 8      | Solid       |
| 9      | 6.0         |
| 10     | 8.8         |
| 11     | Hollow      |
| 12     | 31.4        |
| 13     | 20.0        |
| 14     | 13.7        |
| 15     | 29.9        |

A small scale parameter study was completed for 3D printing primary wicks using an EOS M280 DMLS machine. The EOS M280 has a build volume of 250 x 250 x 325mm which is large enough to print full scale primary wicks and also potentially secondary wicks and compensation chambers. For the optimization study cylindrical wicks 25mm in length and 13mm in diameter were printed using 316LSS. The parts had a 1.0mm thick fully dense shell surrounding the porous center. A total of 15 wicks were printed each with a different parameter set. The pore radius of each sample was measured using the bubble test. For the bubble test one end of the wick was submerged in methanol while the other side was attached to a line of pressurized nitrogen. The nitrogen pressure was increased until a steady stream of bubbles was detected passing through the wick. The pore radius was then calculated using Eq. 1

$$R_p = \frac{2\sigma}{P_b} \quad (1)$$

where  $R_p$  is the pore radius,  $\sigma$  is the surface tension of the fluid used, and  $P_b$  is the bubble point pressure. The results are presented in Table 1. Samples 5 and 11 are labeled as being hollow because the laser power was not sufficient to sinter the metal powder together. Samples 6, 7, and 8 are labeled as solid because the laser power was too high and a fully dense part was made. Several parameter sets successfully produced wicks with pore radii less than 10μm which provides enough capillary pressure for a LHP in the desired 100-200W range. Sample 2 achieved the smallest pore size. Therefore, the DMLS parameter set used for Sample 2 was chosen for fabrication of the full scale primary wicks used for fabrication of the LHP prototype.

The permeability of Sample 2 was also measured. Permeability affects the pressure drop of the liquid through the primary wick. The measurement completed by pumping methanol through the wick and recording the corresponding flow rate and pressure drop. Permeability was then calculated using Darcy's Law. In Figure 4 the permeability of Sample 2 is plotted in comparison to the Anderson Curve. The Anderson Curve relates the permeability to pore radius for sintered wicks. The 3D printed sample had a lower than expected permeability which will result in a higher liquid return pressure drop through the primary wick. However, the primary wick can still be designed so that the liquid pressure drop through the primary wick is small relative to the capillary pressure allowing for successful LHP operation. Further investigation is required to determine why 3D printed wicks have lower permeabilities than traditionally sintered wicks.

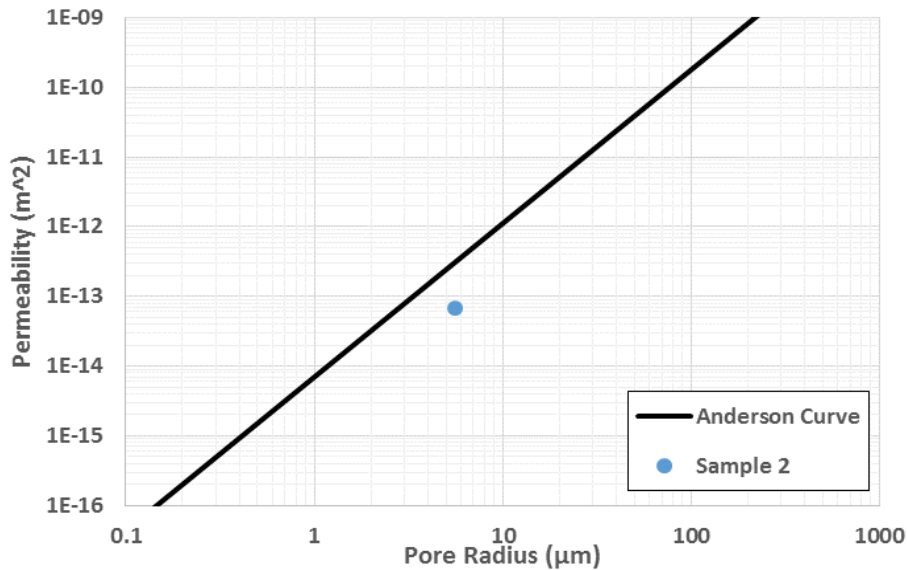


**Figure 4. Permeability of Sample 2 compared to expected permeability (Anderson Curve).**

## B. Secondary Wick

The ability to 3D print secondary wicks would allow for one step fabrication of the entire LHP evaporator. Since secondary wicks have much larger pore sizes to minimize pressure drop a different DMLS parameter set must be used. A small scale parameter study was completed with the goal of producing a wick with a pore radius of approximately 50 $\mu\text{m}$ . To accomplish this the laser spacing was increased from that used for primary wick fabrication. Using different DMLS parameter sets, four secondary wick samples were manufactured and tested. The pore size of each sample was measured using the bubble test as shown in Table 2. The pore size did not increase from the primary wick samples even though the laser spacing was increased. A magnified image of the wick was taken as shown in Figure 5 to better understand why the pore size did not increase. Based on the 100 $\mu\text{m}$  scale bar the majority of the pores do seem to be on the order of a 50 $\mu\text{m}$  radius, but the pores are not continuous. There are sections where metal powder was sintered together inside of the pores. This explains why the measured pore size was similar to the primary wick pore samples. Further work is required to identify a suitable DMLS parameter set for fabrication of secondary wicks. In future testing the laser spacing will be further increased, and potentially a lattice structure could be used for these coarser wicks.

**Table 2. Secondary Wick Samples**

| Parameter Set | Pore Radius   |
|---------------|---------------|
|               | $\mu\text{m}$ |
| 1             | 5.6           |
| 2             | 5.8           |
| 3             | 5.5           |
| 4             | 5.0           |

Larger pores blocked off resulting in smaller measured pore size

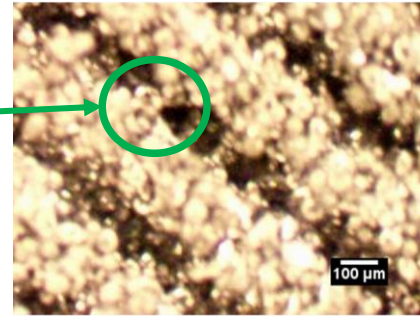


**Figure 5. 3D printed secondary wicks which appear to have 50 $\mu\text{m}$  pores, but are blocked off at sections resulting in measurements of pores less than 10 $\mu\text{m}$ .**

## IV. Scaling Study

The DMLS parameter studies completed for both primary and secondary wicks used small scale test pieces which were 25mm long and 13mm in diameter. The first LHP prototype contains a wick which is 100mm long and 25mm in diameter. Therefore, a scaling study

was completed to determine if the DMLS wick properties are affected by any scaling effects such as increased thermal stresses during fabrication. A total of 12 primary wick samples were printed using parameter set 2. The wick length was varied from 25mm to 50mm and the diameter was varied from 13mm to 25mm. The pore size of each sample was measured for comparison. The results of the scaling study are compiled in Table 3. The pore radius measured for all samples was 5-7 $\mu\text{m}$ . This demonstrates that increasing the size of 3D printed wicks does not have any adverse effects on pore properties from increased thermal stresses. The parameter sets developed based on small scale testing can be applied to full scale primary wicks without any adjustments necessary.

**Table 3. Scaling Study Results**

| Sample |   | Length (mm) | Diameter (mm) | Pore Radius ( $\mu\text{m}$ ) |
|--------|---|-------------|---------------|-------------------------------|
| 1      | A | 25          | 13            | 5.6                           |
|        | B | 25          | 13            | 5.8                           |
| 2      | A | 51          | 13            | 5.7                           |
|        | B | 51          | 13            | 5.8                           |
| 3      | A | 25          | 19            | 6.5                           |
|        | B | 25          | 19            | 6.7                           |
| 4      | A | 51          | 19            | 5.8                           |
|        | B | 51          | 19            | 6.9                           |
| 5      | A | 25          | 26            | 6.4                           |
|        | B | 25          | 26            | 5.5                           |
| 6      | A | 51          | 26            | 6.9                           |
|        | B | 51          | 26            | 6.7                           |



## V. LHP Prototype

A proof of concept prototype was built and tested to verify performance of the 3D printed primary wick. The design was largely based on previous work. Note that significant improvements to the evaporator design can be made through an optimization study for overall reductions in volume and thermal resistance.

### A. Fabrication

The primary wick was designed to be 25mm in diameter, which is a standard size, and 100mm in length to fit inside of a 6U CubeSat. The primary wick must have vapor grooves, a hole for insertion of the secondary wick and liquid return bayonet tube, and a fully dense outside envelope. The fully dense envelope prevents backflow of vapor from the evaporator to the compensation chamber without the use of a knife-edge seal. The primary wick is printed with a thick envelope which is then machined down to create a smooth surface for better contact with the aluminum saddle to reduce thermal resistance. Welding joints have been implemented into the design on both sides for direct welding to the vapor end cap and compensation chamber, eliminating the knife-edge seal and bimetallic joints.

A picture of a 3D printed primary wick is shown in Figure 6. A total of 2 wicks were printed using 316LSS. The primary wicks were helium leak checked and had a leak rate less than  $5 \times 10^{-9}$  std cc/s, which is ACT's requirement for ammonia LHPs. This is a major accomplishment since the primary wick envelope must be hermetic for long term



Figure 6. 3D printed primary wick

use on a satellite. The pore radius of the primary wicks was measured to be  $7 \mu\text{m}$ . This matches the expected pore size based on the small scale testing, and verifies that the wick properties are not effected by scale-up of the part.

A picture of the completed LHP prototype is shown in Figure 7. The condenser tubing length is 3.2m to replicate the length required on a deployable radiator. The entire LHP was helium leak checked and had a leak rate less than  $5 \times 10^{-9}$  std cc/s. The LHP assembly was proof pressure tested with methanol up to 600psi which is twice the pressure of ammonia at the maximum operating temperature of  $50^\circ\text{C}$ . The methanol was then baked out and the LHP was charged with 40g of ammonia which is enough to completely submerge the secondary wick during startup with gravity.

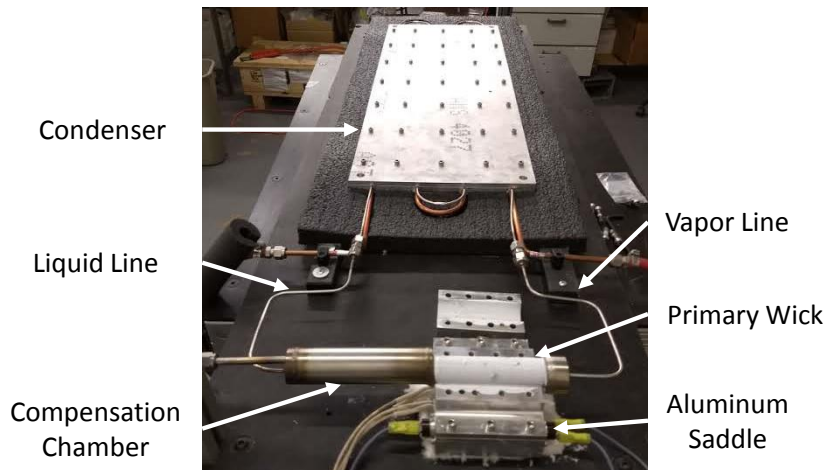
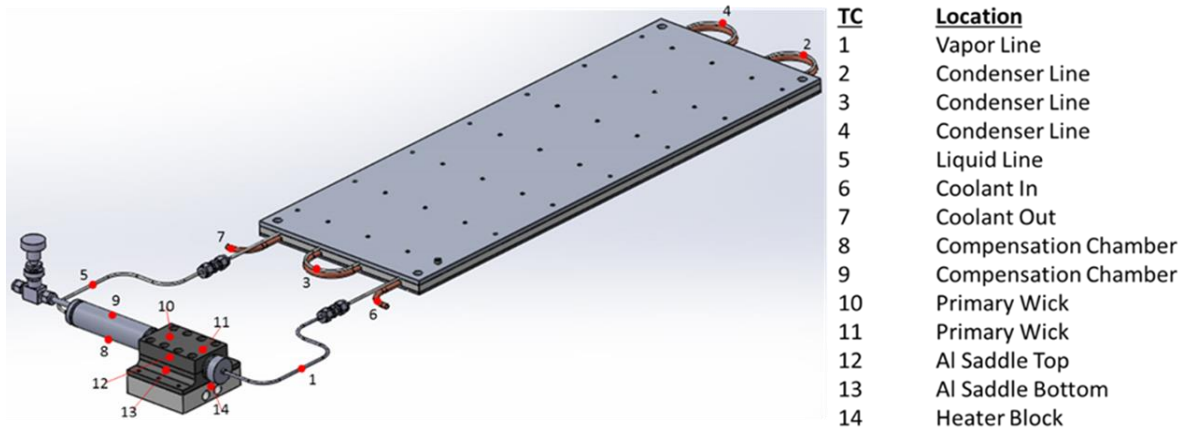


Figure 7. Complete LHP prototype as fabricated

### B. Experimental Testing

A schematic of the thermocouple locations for testing the LHP is shown in Figure 8. Insulation was added to minimize heat losses from the evaporator and heat leak into the condenser. The coolant temperature was set to  $21^\circ\text{C}$

to minimize the effects of heat leak from the environment. For safety, an over temp controller monitored the temperature of the heater block and would shut off power if a temperature of 50°C was exceeded. Additionally two thermostats were wired in series with the cartridge heaters in the heater block which would cut power if a temperature of 50°C was exceeded. The evaporator was raised 13mm above the condenser to ensure that the prototype would operate as LHP and not as a thermosyphon.



**Figure 8. Thermocouple locations used for LHP testing**

### C. Results

A plot of the LHP prototype test results is shown in Figure 9. Startup occurred almost instantly at a power input of 110W. This can be seen by the vapor line temperature increasing above ambient after the power was turned on indicating that vapor is flowing from the wick through the vapor line to the condenser. Steady state was successfully reached at powers of 110, 115, 120, and 125W. This was 2.8x higher than the 45W maximum power observed on the first generation 3D printed LHP prototype. The increase in power is due to the reduction in pore size of the 3D printed primary wick from 44µm to 7µm. This significantly increases the available capillary pressure. At a power of 130W the temperature of the evaporator continued to increase slowly, and did not reach a steady state value. This indicates that dry-out of the primary wick had occurred.

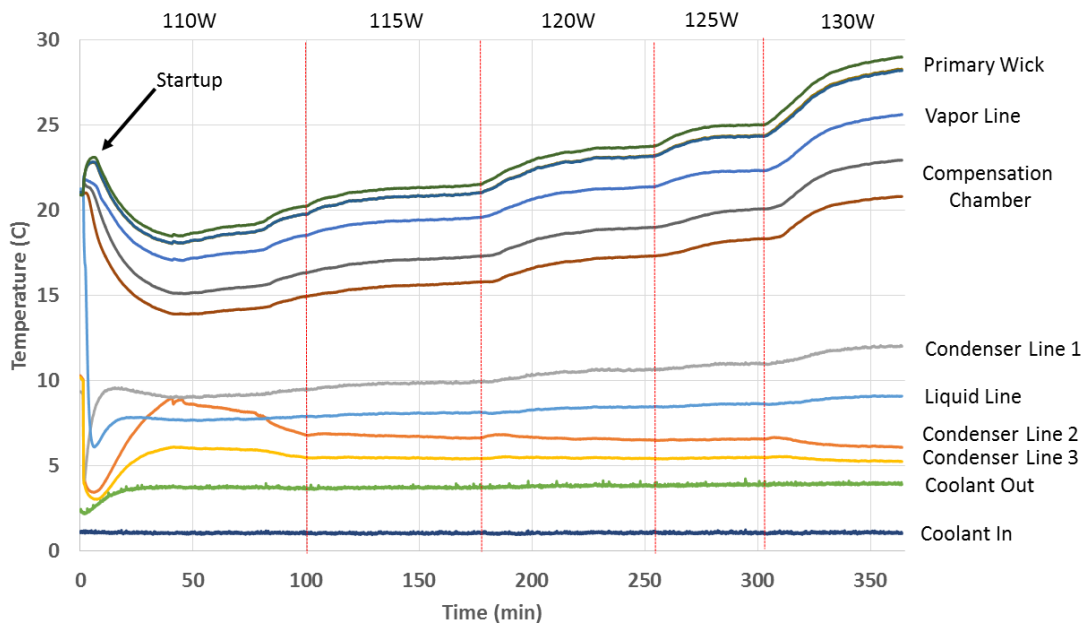


**Figure 9. Plot of LHP testing results showing steady state operation at power levels up to 125W**

## VI. Conclusion

Significant progress has been made in the development of 3D printed LHP evaporators. Previously primary wicks were 3D printed with pore radii of 44 $\mu$ m limiting the maximum LHP power to 45W. Through a more comprehensive DMLS parameter study for optimization of wick fabrication a pore radius of 7 $\mu$ m was achieved. This resulted in an over 50% improvement in maximum power to 125W. There is additional room for improvement in the design of the primary wick. In future work the vapor grooves will be optimized to reduce thermal resistance and pressure drop. Also, progress has been made on 3D printing of secondary wicks as well. Once the secondary wick parameter study is completed the ability to 3D print an entire LHP evaporator will offer significant cost savings. Based on these results, the use of DMLS for fabrication of LHP evaporators is a viable option for CubeSats and other small satellite applications. The ability to scale up the 3D printed wicks without any adverse effects on pore properties was verified making application to larger scale systems possible as well.

## Acknowledgments

This work was funded by NASA through the Small Business Innovation Research (SBIR) program under contract NNX17CM09C. The technical monitor is Dr. Jeff Farmer.

## References

<sup>1</sup>Anderson, W.G., Dussinger, P.M., Garner, S.D., Hartenstine, J.R., and Sarraf, D.B., "Loop Heat Pipe Design, Manufacturing, and Testing – An Industrial Perspective," ASME 2009 Heat Transfer Summer Conference, San Francisco, CA, July 19-23, 2009.

<sup>2</sup>Ku, Jentung. *Operating characteristics of loop heat pipes*. No. 1999-01-2007. SAE Technical Paper, 1999.